

1.5 μm orthogonally polarized dual-output heralded single photon source based on optical fibers with birefringence

Tianyi Ma, Qiang Zhou, Wei Zhang,* Yidong Huang, Xiaowei Cui, Mingquan Lu and Bingkun Zhou

Department of Electronic Engineering, Tsinghua University, Tsinghua National Laboratory for Information Science and Technology, Beijing 100084, China

*zwei@tsinghua.edu.cn

Abstract: In this paper, a heralded single photon source (HSPS) at 1.5 μm with two independent orthogonally polarized outputs is realized based on a piece of polarization maintaining dispersion shifted fiber (PM-DSF). The HSPS is based on two scalar spontaneous four wave mixing (SFWM) processes along the two fiber polarization axes, while two vector SFWM processes are suppressed due to the high birefringence in the PM-DSF. The preparation efficiencies of the two independent outputs are about 73.7% and 69.1%, respectively, under a second-order correlation function $g^{(2)}(0)$ of 0.059. The indistinguishability between the two independent heralded single photons is demonstrated by Hong-Ou-Mandel (HOM) interference with a visibility of 78.9%, showing its great potential in quantum optics experiments and applications of quantum information.

©2013 Optical Society of America

OCIS codes: (270.5585) Quantum information and processing ; (190.4370) Nonlinear optics, fibers; (260.1440) Birefringence

References and links

1. D. Bouwmeester, J. W. Pan, K. Mattle, H. Weinfurter, and A. Zeilinger, "Experimental quantum teleportation," *Nature* **390**(6660), 575–579 (1997).
2. E. Knill, R. Laflamme, and G. J. Milburn, "A scheme for efficient quantum computation with linear optics," *Nature* **409**(6816), 46–52 (2001).
3. V. Giovannetti, S. Lloyd, and L. Maccone, "Quantum metrology," *Phys. Rev. Lett.* **96**(1), 010401 (2006).
4. S. Fasel, O. Alibart, S. Tanzilli, P. Baldi, A. Beveratos, N. Gisin, and H. Zbinden, "High-quality asynchronous heralded single-photon source at telecom wavelength," *New J. Phys.* **6**, 163 (2004).
5. O. Alibart, D. B. Ostrowsky, P. Baldi, and S. Tanzilli, "High-performance guided-wave asynchronous heralded single-photon source," *Opt. Lett.* **30**(12), 1539–1541 (2005).
6. T. B. Pittman, B. C. Jacobs, and J. D. Franson, "Heralding single photons from pulsed parametric down-conversion," *Opt. Commun.* **246**(4-6), 545–550 (2005).
7. S. D. Dyer, M. J. Stevens, B. Baek, and S. W. Nam, "High-efficiency, ultra low-noise all-fiber photon-pair source," *Opt. Express* **16**(13), 9966–9977 (2008).
8. C. Söller, O. Cohen, B. J. Smith, I. A. Walmsley, and C. Silberhorn, "High-performance single-photon generation with commercial-grade optical fiber," *Phys. Rev. A* **83**(3), 031806 (2011).
9. M. Fiorentino, P. L. Voss, J. E. Sharping, and P. Kumar, "All-fiber photon-pair source for quantum communications," *IEEE Photon. Technol. Lett.* **14**(7), 983–985 (2002).
10. H. Takesue and K. Inoue, "1.5- μm band quantum-correlated photon pair generation in dispersion-shifted fiber: suppression of noise photons by cooling fiber," *Opt. Express* **13**(20), 7832–7839 (2005).
11. E. A. Goldschmidt, M. D. Eisaman, J. Fan, S. V. Polyakov, and A. Migdall, "Spectrally bright and broad fiber-based heralded single-photon source," *Phys. Rev. A* **78**(1), 013844 (2008).
12. Q. Zhou, W. Zhang, J. R. Cheng, Y. D. Huang, and J. D. Peng, "Polarization-entangled bell states generation based on birefringence in high nonlinear microstructure fiber at 1.5 μm ," *Opt. Express* **34**, 2706–2708 (2009).
13. Q. Zhou, W. Zhang, J. R. Cheng, Y. D. Huang, and J. D. Peng, "Properties of optical fiber based synchronous heralded single photon sources at 1.5 μm ," *Phys. Rev. A* **375**, 2274 (2011).
14. P. X. Wang, Q. Zhou, W. Zhang, Y. D. Huang, and J. D. Peng, "High-quality fiber-based heralded single-photon source at 1.5 μm ," *Chin. Phys. Lett.* **29**(5), 054215 (2012).

15. W. Zhang, Q. Zhou, J. R. Cheng, Y. D. Huang, and J. D. Peng, "Impact of fiber birefringence on correlated photon pair generation in highly nonlinear microstructure fibers," *Eur. Phys. J. D* **59**(2), 309–316 (2010).
 16. H. Takesue, "1.5- μm band Hong-Ou-Mandel experiment using photon pairs generated in two independent dispersion shifted fibers," *Appl. Phys. Lett.* **90**(20), 204101 (2007).
 17. X. Li, L. Yang, L. Cui, Z. Y. Ou, and D. Yu, "Observation of quantum interference between a single-photon state and a thermal state generated in optical fibers," *Opt. Express* **16**(17), 12505–12510 (2008).
 18. H. R. Brown and R. Q. Twiss, "A test of a new type of stellar interferometer on Sirius," *Nature* **178**(4541), 1046–1048 (1956).
 19. C. K. Hong, Z. Y. Ou, and L. Mandel, "Measurement of subpicosecond time intervals between two photons by interference," *Phys. Rev. Lett.* **59**(18), 2044–2046 (1987).
 20. P. Grangier, G. Roger, and A. Aspect, "Experimental evidence for a photon anticorrelation effect on a beam splitter: a new light on single-photon interferences," *Europhys. Lett.* **1**(4), 173–179 (1986).
-

1. Introduction

1.5 μm single photon sources play important roles in applications of quantum communication and quantum information processing [1–3]. The traditional way to obtain single photons is based on the attenuated coherent light pulses. Physically the photon number in an attenuated coherent light pulse satisfies the Poisson distribution, the average photon number in the pulse should be attenuated to a level far lower than 1 to reduce the possibility of multi-photon events, leading to a low single photon generation efficiency. Hence, the performance of attenuated coherent light pulses is limited by the trade-off relation between the efficiency and the multi-photon level. Heralded single-photon sources (HSPSs) [4, 5] hold the promise to overcome the intrinsic problem of the attenuated coherent light pulses. The HSPS is based on the generation of correlated photon pair by spontaneous optical nonlinear parametric processes, in which one photon of the correlated photon pair is detected, providing an electrical trigger signal to herald the arrival of the other photon.

Two kinds of nonlinear parametric processes are employed to realize 1.5 μm correlated photon pair generation. One is spontaneous parametric down-conversion process in nonlinear bulk crystals [6] or periodically poled crystal waveguides. The other is spontaneous four wave mixing (SFWM) in the third order nonlinear waveguides, such as optical fibers [7–10] and silicon wire waveguides. Recently, fiber based 1.5 μm correlated photon pair generation focused more and more attention, which is based on commercial optical fibers and fiber-based components, compatible with current techniques of optical fiber networks. Suppressing the spontaneous Raman scattering by fiber cooling technique, high quality correlated photon pairs generation has been realized in several types of fibers, such as dispersion shifted fibers, high nonlinearity fibers and micro-structured fibers [11, 12]. By optimizing the fiber selection, pump level and filtering frequency of the signal and idler photons, a fiber based HSPS with a preparation efficiency of $\sim 80\%$ was demonstrated under a $g^{(2)}(0)$ of 0.06 [13–15]. On the other hand, quantum interferences between the heralded photons generated from two pieces of optical fibers utilizing the pump light from the same source has been demonstrated [16,17], showing their indistinguishability which is required in quantum optics experiments and applications of quantum information. In this paper, a 1.5 μm all-fiber HSPS with two independent orthogonally polarized outputs is proposed and demonstrated. The two independent heralded single photon outputs are realized based on one piece of commercial birefringent fiber, reducing the complexity of the quantum interference experiment between non-classical light. In the experiment, the two heralded photon generation is based on two independent correlated photon pairs, which are obtained through the same one filter and splitting system, eliminating the impact of bandwidth mismatching between the two heralded photons in interference.

The content is structured as follows. The scheme of the orthogonally polarized dual-output HSPS is introduced in section 2 and the experiment setup for it is shown in section 3. The experiment results are discussed in section 4. In subsection 4.1, the independence between the two correlated photon pair generation processes along the two fiber polarization axes is demonstrated. Then the performances of the two heralded single photon outputs are

demonstrated in subsection 4.2. Subsection 4.3 shows the results of quantum interference between the heralded photons from the outputs and discussion is included in subsection 4.4. The conclusion is presented in section 5.

2. Scheme of the orthogonally polarized dual-output HSPS

When a pump light injects into a piece of optical fiber, usually two kinds of SFWM processes will occur shown by Fig. 1, in which the two annihilated photon have the same frequency denoted by ω_p . the two generated photons are denoted by ω_s and ω_i , while ω_s is for the photon with higher frequency. H and V denote the polarization directions corresponding to the fast and slow axes of optical fibers, respectively. One of the SFWM processes is the scalar scattering processes, shown in Fig. 1(a), in which two pump photons polarized along the same fiber polarization axis annihilated, while, a photon pair with the same polarization is generated. The other is the vector scattering processes, shown in Fig. 1(b), in which the two annihilated pump photons polarized in different fiber polarization axis, so do the two photons of the generated photon pair.

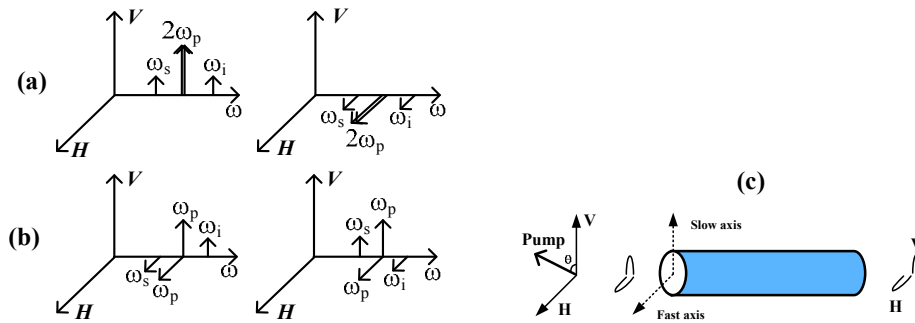


Fig. 1. SFWM processes. (a) Scalar scattering process. (b) Vector scattering process. (c) Two scalar SFWM processes along both axes.

However, things are different in a fiber with high birefringence. Considering that a linearly polarized pulsed pump light injects into a birefringent fiber with a polarization direction of 45° respecting to fiber polarization axes, the two pump components polarized along the two polarization axes will walk off rapidly due to the high birefringence as shown in Fig. 1(c), resulting an effective suppression of vector scattering processes. While, correlated photon pairs with orthogonal polarization directions are generated by the two scalar scattering processes independently. This effect has been utilized to realize polarization entangled photon pair generation in our previous work [15]. In this paper, it is utilized to realize heralded single photon generations along the two fiber polarization axes, respectively, realizing an orthogonally polarized dual-output HSPS.

3. Experiment setup

The experimental setup is based on the commercial fiber components, which is shown in Fig. 2. The part I is the setup of the orthogonally polarized dual-output HSPS. The pulsed pump light with a repetitive frequency of 4.05 MHz is generated from a passive mode locked fiber laser and amplified by an EDFA. Then, by a pump filter system which consists of a distribute fiber grating (FBG), a circulator and fiber dense wavelength division multiplexing (DWDM) devices, a side-band suppression of more than 110 dB is achieved at wavelengths where the signal/idler photon detection is performed. The center wavelength and line width of the pulsed pump light after the filter system are 1552.52 nm and 0.2 nm, respectively. The pulse width is about several tens of picoseconds estimated by the line width. Before the pump light injects into the nonlinear medium, a piece of nonlinear birefringent fiber, a variable optical attenuator (VOA1) is used to control its power level, while a polarizer (P), a rotatable half wave plate

(HWP1) and a polarization controller (PC1) are used to achieve linear polarization and adjust its polarization direction. The nonlinear birefringent fiber used in the experiment is a piece of polarization maintaining dispersion shifted fiber (PM-DSF, fabricated by Fujikura Ltd.). To suppress the noise photons generated by spontaneous Raman scattering, the fiber is cooled by liquid nitrogen. The PM-DSF is 500m in length and spliced to a circulator and a Faraday mirror at its two ends. The pump light injects into the fiber by the port 1 of the circulator, then the two polarization components walk off rapidly. At the other end of the PM-DSF, the pump light reflects by the Faraday mirror, the two polarization components swap and walk together again when the pump light propagates along this direction. Finally the pump light is out of the PM-DSF from port 3 of the circular with the same polarization state of the input pump light, ensuring that the two polarization components are out of the fiber simultaneously. Considering that the birefringence beating length is about 2mm, the two pump polarization components will walk off entirely in several meters, far smaller than the fiber length, hence, vector processes can be effectively suppressed in this process, while the two scalar scattering processes along the two fiber polarization axes generate correlated photon pairs with orthogonal polarization directions independently.

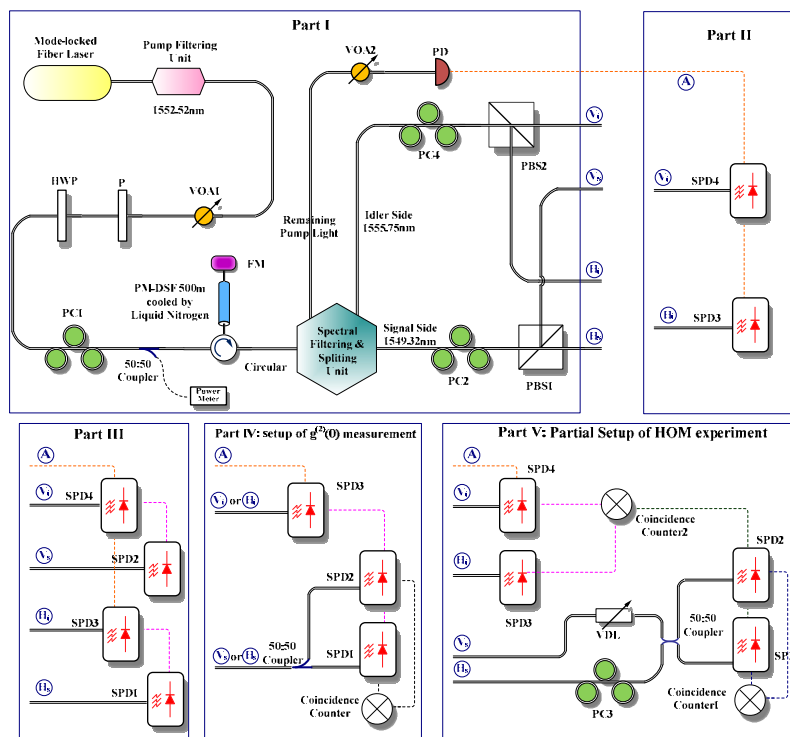


Fig. 2. Experiment Setup. VOA, variable optical attenuator; P, polarizer; HWP, half-wavelength plate; PC, polarization controller; FM, faraday mirror; PBS, polarization beam splitter; PD, photon detector; VDL, variable delay line; SPD, single photon detector; H_i , Idler photons along H-axis; V_s , Idler photons along V-axis; H_s , Signal photons along H-axis; V_s , Signal photons along V-axis.

The signal and idler photons of generated correlated photon pairs and the residual pump light out of the fiber are separated by a filter and splitting system. Since the photon number in a residual pump pulse is far larger than the level of generated correlated photon pairs, high pump photon suppression is required for signal/idler photon detection. The filter and splitting is realized by a DWDM module, which packages 8 DWDM components together without fiber connection between them. This design reduces the transmission loss and improves the

polarization stability of the light propagating through the filter and splitting. The center wavelength and spectral width of selected signal photons are 1549.32 nm and 0.81 nm, respectively, while, 1555.75 nm and 0.85 nm for the idler ones. The total pump suppression is higher than 110 dB at both sides. The idler photons of the correlated photon pairs generated along the fast and slow axes of the PM-DSF are separated by a polarization controller (PC4) and a polarization beam splitter (PBS2) and directed to the output ports denoted by H_i and V_i , respectively. So do the signal photons. The two ports for the signal photons are denoted by H_s and V_s , which are also corresponding to the fast and slow axes of the PM-DSF, respectively. The residual pump light is detected by a photon detector (PD) to provide the trigger signals for the photon counting measurements.

Part II ~Part IV show the photon counting measurement setup for different experiments, which will introduced in detail with the experiment results in section 4. It is worth to note here that the single photon detectors used in the experiments are based on InGaAs/InP avalanche photodiodes (Id201, Id Quantique), and operate in gated Geiger mode with a detection window width of 2.5 ns and a deadtime of 10 μ s. The detection efficiencies and the dark counts of the SPDs are collimated before the experiment and shown in Table 1.

Table 1. Characters of SPDs

	SPD1	SPD2	SPD3	SPD4
Efficiency	15.17%	15.42%	14.05%	14.23%
Dark Count Rates (/gate)	7.79×10^{-5}	6.01×10^{-5}	8.63×10^{-5}	8.49×10^{-5}

4. Experiment results and discussion

4.1 Independence between correlated photon pairs generated along two polarization axes of the PM-DSF

Firstly, the independence between the two correlated photon pair generation processes along the two fiber polarization axes is demonstrated. In this experiment, the pump light is aligned to the H-axis of the PM-DSF. Photon count rates of the two idler side ports, H_i and V_i , under different pump levels are measured by SPD3 and SPD4, respectively, and shown in Fig. 3. The measurement setup of this experiment is shown by the Part II of Fig. 2. In the following experiment results, all the photon count rates are statistical results of five measurements with a counting duration of 30 s.

Figure 3(a) shows the photon generation rates with alignment to the H-axis in the PM-DSF and the measured photon count rates at port H_i , the photon generation rates are calculated from the measured photon count rates with loss of optical path and efficiency of SPDs. It can be seen that, the quadratic term is higher than the constant and linear terms when the total photon generation rates is greater than 0.015 per pulse and dominate at generation rates level of 0.05~0.3, which is the range that the following experiments of HSPS are used. Figure 3(b) shows the photon generation rates with alignment to the V-axis in the PM-DSF and the measured photon count rates at port V_i . It can be seen that the photon generation rates at V_i port is far lower than that at H_i port. Furthermore, the linear term dominates the relation between the photon generation rates and the increasing pump level. Similar results are also demonstrated in the two ports at signal side.

The results of Fig. 3 shows that the pump light polarized along one of the polarization axis of the PM-DSF could realize correlated photon pair generation along this axis by the scalar scattering process, while has little contribution on the correlated photon pair generation along the other fiber axis. The independence of the correlated photon pair generations along the two fiber axes is the base of the orthogonal polarized dual-output of the HSPS utilizing the birefringent fibers.

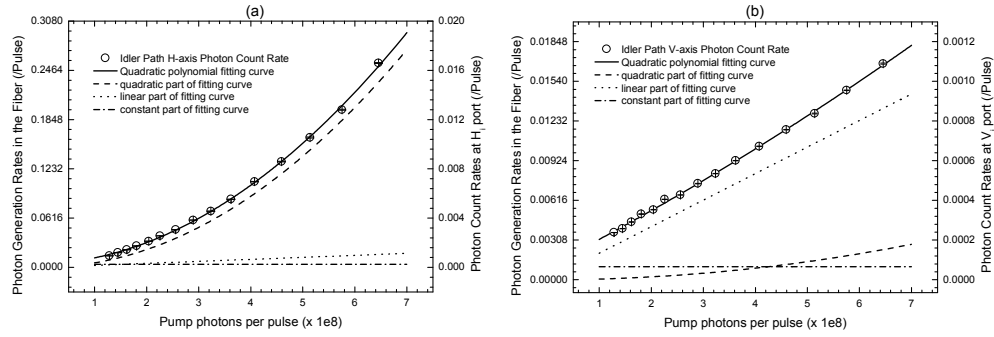


Fig. 3. Photon generation rates and measured photon count rates under different pump levels. (a) Photon count rates at H_i (Idler photons along H-axis) ports. The circles with error bars in the figure are measured photon count rates, which is fitted by a polynomial of $aP^2 + bP + c$, where P is the pump level, a , b and c are the fitting parameters. The fitting result is shown by the solid line. The dash-dot, dot and dash lines in the figure are the fitting results of the constant, linear, and quadratic terms of the fitting polynomial, which represent the contributions of SPD dark counting, noise photons generated by spontaneous Raman scattering or residual pump light and generated correlated photon pairs by the scalar SFWM, respectively. (b) Photon count rates at V_i (Idler photons along V-axis) ports, which are of the same symbol and line definitions as Fig. 3(a).

4.2 Performances of the two orthogonal polarized outputs of the HSPS

Then, the pump polarization direction is rotated to 45° respecting to the fiber polarization axes. In this case, the two pump polarization components have the same intensity and generate correlated photon pairs along the two fiber axes independently with the same rate. The two orthogonal polarized outputs of the HSPS are realized by detecting the idler side photons at H_i and V_i ports to herald the arrivals of signal side photons at H_s and V_s ports.

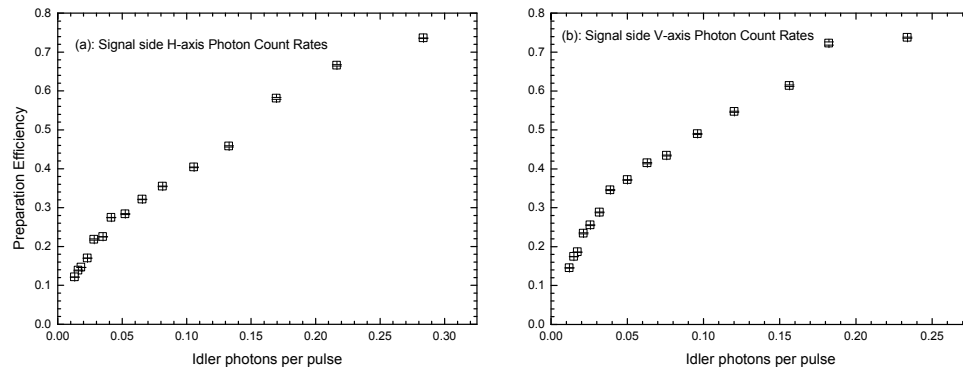


Fig. 4. Measured preparation efficiencies under different idler photon generation rates. (a) Preparation efficiencies at H_s (Signal photons along H-axis) ports. (b) Preparation efficiencies at V_s (Signal photons along V-axis) ports.

The measurement setup for the preparation efficiencies of the two orthogonal polarization outputs is shown in Part III of Fig. 2. The photons of H_i port is detected by the SPD3 utilizing the detected residual pump pulse as the trigger signal. The port H_s is one of the HSPS output, which is detected by SPD1 utilizing the output signal of the SPD3 as the heralding signal. The other output of the HSPS is the port of V_s , which is detected by the SPD2 utilizing the output signal of SPD4 as the heralding signal. SPD4 is used to detect the photons of port V_i .

Figure 4 is the measured preparation efficiencies of the two ports for the heralded single photon generation under different idler photon generation rates. The result of port H_s is shown

in Fig. 4(a), which is calculated by the ratio between the count of SPD1 and the count of SPD3. The results of port V_s is calculated by the ratio between the counts of SPD2 and SPD4 and shown in Fig. 4(b). It can be seen that for both ports the preparation efficiencies rise monotonously with the increasing idler photon generation rate. At low trigger rate, noise photons generated by the spontaneous Raman scattering and residual pump light worsen the preparation efficiencies a lot. While, as the idler photon generation rate increases with the pump level, the contribution of correlated photon pair dominates, improving the preparation efficiencies. On the other hand, since the correlated photon pair generation satisfies the thermal statistical distribution, multi-pair events cannot be neglected when the idler photon generation rate is above some threshold, which leads to the further rise of the measured preparation efficiencies with the increasing trigger rate. However, multi-pair events increase the multi-photon possibility so as to limit the quality of the heralded single photon output.

The multi-photon possibilities of the heralded single photon output can be evaluated by the measurement of the second-order correlation degree $g^{(2)}(0)$. The Hanbury Brown–Twiss setup [18] for the measurement of $g^{(2)}(0)$ at the port H_s is shown in the Part IV of Fig. 2. SPD3 detects the photons from port H_i to give the heralding signal for the port H_s . The photons of port H_s are separated by a 50:50 fiber coupler and detected by SPD1 and SPD2, respectively, utilizing the heralding signal as their triggers. $g^{(2)}(0)$ can be calculated by $g^{(2)}(0) = N_{\infty} / (N_1 N_2)$, where N_1 and N_2 are the photon counts of SPD1 and SPD2, respectively, while N_{co} is their coincidence count. Similar setup is also used to measure the $g^{(2)}(0)$ at the port V_s .

Figures 5(a) and 5(b) are the measured $g^{(2)}(0)$ of the port H_s and V_s under different idler photon generation rates, respectively. It can be seen that for both ports, the $g^{(2)}(0)$ also increases with the increasing idler photon generation rate. Hence, the pump level should be optimized to take trade-off between the preparation efficiency and $g^{(2)}(0)$ of the HSPS. Under a $g^{(2)}(0)$ of 0.059, the preparation efficiencies of the two independent outputs are 73.7% and 69.1%, respectively. While, the idler photon generation rates of H-axis and V-axis are 0.241 and 0.238, respectively.

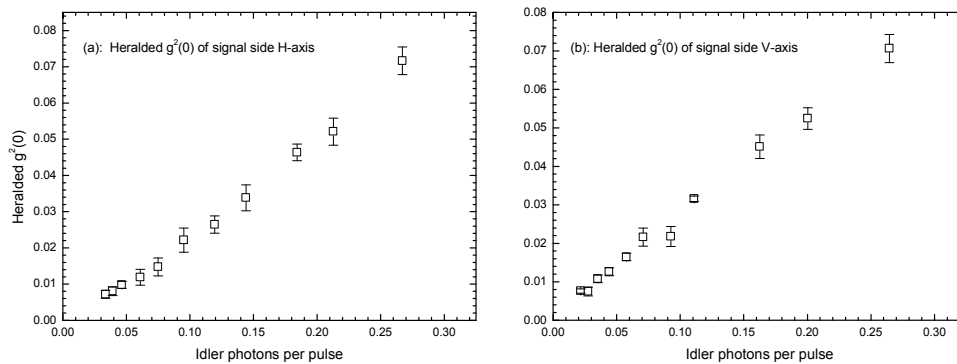


Fig. 5. Measured $g^{(2)}(0)$ under different idler photon generation rates. (a) $g^{(2)}(0)$ at H_s (Signal photons along H-axis) ports. (b) $g^{(2)}(0)$ at V_s (Signal photons along V-axis) ports.

4.3 Indistinguishability between the heralded photons of the two independent ports

The Hong-Ou-Mandel (HOM) interference experiment [19, 20] is taken to demonstrate the indistinguishability between the heralded photons of the ports H_s and V_s . The measurement setup for this experiment is shown in the Part V in Fig. 2. The SPD3 and SPD4 are used to detect the photons of port H_i and V_i , respectively. Their coincidence count provides a heralding signal that both port H_s and V_s generate photons, simultaneously. The heralded photons at port H_s and V_s inject into a 50:50 fiber coupler and detected by SPD1 and SPD2

(triggered by the heralding signal) at the output ports of the coupler. The polarization controller (PC3) before the fiber coupler is used to ensure that the heralded photons from port H_s and V_s have the same polarization. The variable delay line (VDL) before the fiber coupler is used to adjust the difference of the times when the heralded photons of the two ports arrive at the fiber coupler.

Figure 6(a) shows the coincidence count of the SPD1 and SPD2 with different time delay of the VDL when the idler correlated photon pair generation rates in the fiber is 0.187 per pulse. Since SPD1 and SPD2 are triggered by the coincidence count of the SPD3 and SPD4, it is actually a 4-fold photon coincidence count for the four ports of the sources (H_s , V_s , H_i and V_i). It can be seen that a clear dip of HOM interference appears when the time delay of the VDL is adjusted to a proper value to realize the simultaneous arrival of the heralded photons of the two ports. The indistinguishability between the two heralded photons can be evaluated by the visibility of the dip. Since the filter spectra for the signal and idler photons in the experiment setup can be well approximated by a Gaussian function, the shape of the HOM dip can be fitted with the following function [9],

$$N_c = C_0 \left(1 - V_{\text{HOM}} e^{-0.5(\Delta T^{-1} \Delta L / c)^2} \right) \quad (1)$$

and shown in Fig. 6(a) as the solid line. Where, C_0 is the coincidence counts without HOM interference, V_{HOM} is the visibility of the dip, ΔT is the width of the pump pulse, c is the light speed in vacuum, and ΔL is the light path difference of the heralded photons from the two ports. The center of the dip is corresponding to $\Delta L = 0$. It can be seen that V_{HOM} in Fig. 6(a) is more than 62.5% with 95% confidence bounds without subtraction of background noise. V_{HOM} can be farther improved by reducing the pump level to suppress the possibility of multi-pairs events. Figure 6(b) shows the coincidence count of the SPD1 and SPD2 without subtraction of background noise when the correlated photon pair generation rates in the fiber for the H_i port is 0.0048 per pulse. Fitting with Eq. (1), the visibility of fitted curve V_{HOM} in Fig. 6(b) is more than 78.9% with 95% confidence bounds, indicating obvious indistinguishability between the heralded single photons of the two ports.

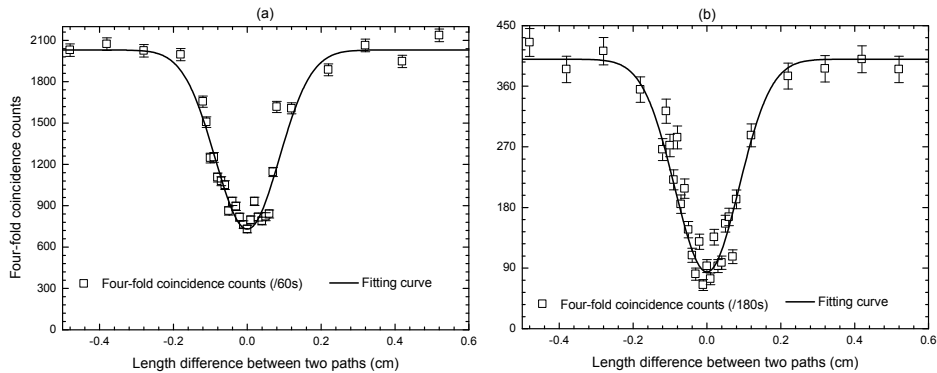


Fig. 6. Results of HOM interference between the heralded photons of ports H_s and V_s as a function of length difference between two paths. (a) Result with 60s accumulation when idler photon generation rates is 0.187 per pulse. (b) Result with 180s accumulation when idler photon generation rates is 0.0048 per pulse.

4.4 Discussion

The scheme proposed in this paper has some advantages on realizing $1.5\mu\text{m}$ HSPSs and observing their quantum interference. In this scheme, two output ports of HSPS are based on one PM-DSF and share the same filter and splitting system for their signal and idler photons. It not only simplifies the experiment setup for the HOM interference experiment, but

guarantees that the two ports have the same output photon spectrum, which is helpful to improve the indistinguishability of the output single photons of the two ports.

On the other hand, this scheme is more robust to the environment variation. It is well known that changes of environment temperature and stress on the fiber would lead to the polarization state variation when light propagates through a fiber without birefringence. Hence, in many reported interference experiments of fiber-based quantum light source [16] [17], although polarization controllers are used to collimate the polarization of the photons, their long term performance is doubtful due to the impact of environment variation. In the scheme proposed in this work, the output photons for each port are generated in one specific polarization axis of the PM fiber. Although polarization controllers are used in the parts of pump source and interference measurement, the experiment setup has potential on developing all polarization maintaining dual-output HSPS to realize long term operation.

5. Conclusion

As a kind of fundamental quantum devices, 1.5 μm HSPSs have important applications in quantum communication and quantum computing. In this paper, one kind of all fiber HSPS at 1.5 μm band with two independent orthogonally polarized outputs is realized, which is based on the suppression of vector SFWM processes in a piece of PM-DSF due to its high birefringence. The preparation efficiencies of the two independent outputs are 73.7% and 69.1%, respectively, under a $g^{(2)}(0)$ of 0.059. The HOM interference experiment between the heralded photons of the two ports is carried out and shows a HOM dip visibility of 78.9% without subtraction of background noise, which demonstrates the indistinguishability between the heralded single photons generated by the two orthogonal polarized output ports.

Acknowledgments

This work is supported in part by 973 Programs of China under Contract No. 2011CBA00303 and 2010CB327606, Tsinghua University Initiative Scientific Research Program, Basic Research Foundation of Tsinghua National Laboratory for Information Science and Technology (TNList), and China Postdoctoral Science Foundation.